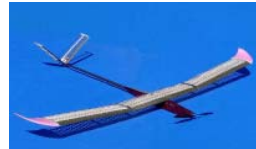
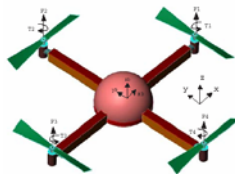




Autonomous Systems Laboratory



Dynamic Modeling of UAVs

(Unmanned Aerial Vehicles)

S. Bouabdallah, A. Noth and R. Siegwart

Version 2.0

05/2006

1 Introduction

Dynamic modeling is an important step in the development and the control of a dynamic system. In fact, the model allows the engineer to analyze the system, its possibilities and its behavior depending on various conditions. Moreover, dynamic models are widely used in control design.

This is especially important for aerial robots where the risk of damage is very high as a fall from a few meters can seriously damage the platform. Thus, the possibility to simulate and tune a controller before implementing it on the real machine is highly appreciable.

This course is structured into two simplified examples of dynamic modeling of:

- A four-rotors model helicopter (Quadrotor) in hover that will be modeled with **Newton-Euler formalism**.
- A lightweight model airplane for which the **Lagrange-Euler formalism** will be used.

1.1 Objectives

The main objective of this course is to introduce the modeling of unmanned aerial vehicles through two examples used in research. The second objective is to make the reader aware of the importance of modeling for engineers, especially for controlling systems. The two models presented below are derived for system's analysis, control-law design and simulation. Fig. 1 shows a situation where a model is used for control design.

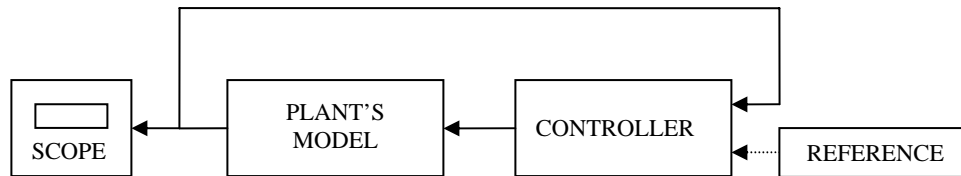


Figure 1: Control simulation bloc diagram

2 Orientation of the UAV

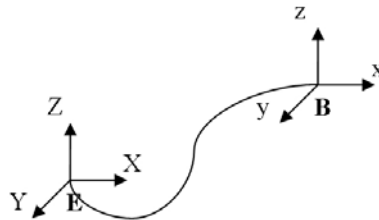


Figure 2: General Coordinate System

Let's consider Earth fixed frame $E = \{E_x, E_y, E_z\}$ and body fixed frame $B = \{E_x, E_y, E_z\}$ on the UAV. At each moment, we need to know the position and the orientation of B relative to E.

2.1.1 Rotation Parameterization

The rotation of a rigid body in space can be parameterized using several methods (Euler angles, quaternion, Tait-Bryan angles ...).

Tait-Bryan angles also called “Cardano angles” are extensively used in aerospace engineering where they are called “Euler angles”. This conflicts with the real usage of “Euler angles” which is a mathematical representation of three successive rotations about different possible axes which are often confused in literature [11].

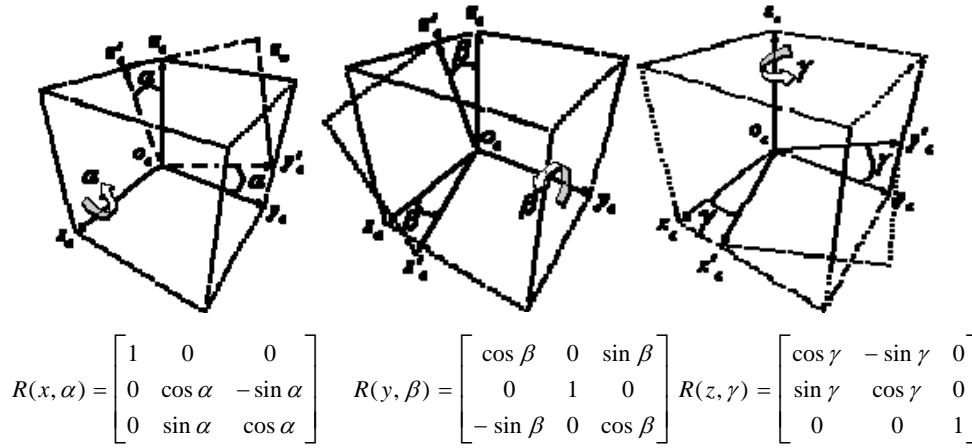


Figure 3: Successive rotations in roll, pitch and yaw according to Tait-Bryan convention

In this document, we use Tait-Bryan angles to describe the orientation of our UAVs. It consists of three successive rotations:

- Rotation of ϕ around \vec{x} : **roll** ($-\pi < \phi < \pi$)
- Rotation of θ around \vec{y} : **pitch** ($-\pi/2 < \theta < \pi/2$)
- Rotation of ψ around \vec{z} : **yaw** ($-\pi < \psi < \pi$)

The complete rotation matrix, called *Direct Cosine Matrix* is then [5]:

$$R(\phi, \theta, \psi) = R(z, \psi) \cdot R(y, \theta) \cdot R(x, \phi)$$

$$R(\phi, \theta, \psi) = \begin{bmatrix} \cos \psi & -\sin \psi & 0 \\ \sin \psi & \cos \psi & 0 \\ 0 & 0 & 1 \end{bmatrix} \cdot \begin{bmatrix} \cos \theta & 0 & \sin \theta \\ 0 & 1 & 0 \\ -\sin \theta & 0 & \cos \theta \end{bmatrix} \cdot \begin{bmatrix} 1 & 0 & 0 \\ 0 & \cos \phi & -\sin \phi \\ 0 & \sin \phi & \cos \phi \end{bmatrix}$$

$$R(\phi, \theta, \psi) = \begin{bmatrix} \cos \psi \cos \theta & \cos \psi \sin \theta \sin \phi - \sin \psi \cos \phi & \cos \psi \sin \theta \cos \phi + \sin \psi \sin \phi \\ \sin \psi \cos \theta & \sin \psi \sin \theta \sin \phi + \cos \psi \cos \phi & \sin \psi \sin \theta \cos \phi - \sin \psi \cos \phi \\ -\sin \theta & \cos \theta \sin \phi & \cos \theta \cos \phi \end{bmatrix} \quad (1)$$

2.1.2 Angular rates

The time variation of Tait-Bryan angles (ϕ, θ, ψ) is a discontinuous function. Thus, it is different from body angular rates (p, q, r) ¹ which are physically measured with gyroscopes for instance.

In general, an Inertial Measurement Unit (IMU) is used to measure the body rotations and directly calculate for the Tait-Bryan angles.

We can get [8]:

$$\begin{bmatrix} p \\ q \\ r \end{bmatrix} = R_r \begin{bmatrix} \dot{\phi} \\ \dot{\theta} \\ \dot{\psi} \end{bmatrix} \quad (2)$$

Where:

$$R_r = \begin{bmatrix} 1 & 0 & -\sin \theta \\ 0 & \cos \phi & \sin \phi \cos \theta \\ 0 & -\sin \phi & \cos \phi \cos \theta \end{bmatrix} \quad (3)$$

However, Tait-Bryan angles representation suffer from a singularity ($\theta = \pm\pi/2$) also known as the “gimbal lock”. In practice, this limitation does not affect the UAV in normal flight mode.

3 The Quadrotor example

3.1 Quadrotor concept

The Quadrotor concept has been around for a long time. The Breguet-Richet Quadrotor helicopter “Gyroplane No.1” built in 1907 is reported to have lifted into flight. One can describe the vehicle as having four propellers in cross configuration. The two pairs of propellers (1, 3) and (2, 4) as described in Fig. 2, turn in opposite directions. By modifying the rotor speed, one can change the lift force and create motion. Thus, increasing or decreasing the speed of the four propellers together generates vertical motion. Changing the speed of the propellers 2 and 4 conversely produces roll rotation coupled with lateral motion. Pitch rotation is obtained similarly by acting on the propellers 1 and 3. Yaw rotation is more subtle as it results from the difference in the counter-torque (drag) between each pair of propellers.

¹ Notation used in aerospace engineering

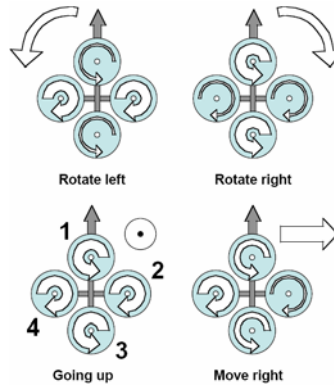


Figure 4: Quadrotor motion description, the arrow width is proportional to the propeller rotational speed

3.2 Grasping the main effects

The helicopter is one of the most complex flying systems ever developed. This is due to the important number of physical effects acting on it as shown in Table 1. It is clear that the complete model of a helicopter is very complex and thus not easy to handle and not suitable for real-time control design. In the same time, the engineer needs to grasp the main effects acting on the system in order to have a faithful representation of its dynamics. Moreover, a model has to be developed according to its purpose. For instance, a simulation model would be more complex than a one for control design.

Effect	Source	Formulation
Aerodynamic effects	- Propeller rotation - Blades flapping	$C\Omega^2$
Inertial counter torques	- Change in propeller rotation speed	$J\dot{\Omega}$
Gravity effect	- Center of mass position	
Gyroscopic effects	- Change in orientation of the rigid body - Change in orientation of the propeller plane	$I\dot{\theta}\psi$ $J\Omega\dot{\theta}, \dot{\phi}$
Friction	- All helicopter motion	$C\dot{\phi}, \dot{\theta}, \dot{\psi}$

Table 1: Main physical effects acting on a helicopter

In this example we develop a model for control design, so we will keep it as simple as possible.

- Earth is supposed flat and stationary in inertial space.
- The helicopter is seen as a single rigid body.
- The effect of the body moments on the translational dynamics is neglected.
- The center of mass and the body fixed frame origin are assumed to coincide.
- The ground effect is neglected.

R

- Friction is only considered on the yaw motion.
- The structure is supposed rigid and symmetric (diagonal inertia matrix).
- The thrust and the drag are supposed proportional to the square of the propeller speed.
- Near hover we can consider (ϕ, θ, ψ) equivalent to (p, q, r) .

3.3 Model derivation using Newton-Euler approach

In this example we consider the helicopter as a single rigid body with 6 degrees of freedom. This body is free to move under the actions of the gravity, gyroscopic moments and aerodynamic forces.

Let's consider Earth fixed frame $E = \{E_x, E_y, E_z\}$ and body fixed frame $B = \{E_x, E_y, E_z\}$.

Using Tait-Bryan angles parameterization, the airframe orientation in space is given by a rotation R from B to E , where $R \in SO(3)$ is the rotation matrix.

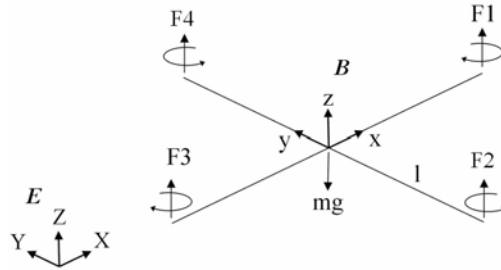


Figure 5: Frame system with body fixed frame B and earth fixed frame E

The dynamics of a rigid body under external forces applied to the center of mass and expressed in the body fixed frame as shown in [2] are in Newton-Euler formalism:

$$\begin{bmatrix} mI_{3 \times 3} & 0 \\ 0 & I \end{bmatrix} \begin{bmatrix} \dot{V} \\ \dot{\omega} \end{bmatrix} + \begin{bmatrix} \omega \times mV \\ \omega \times I\omega \end{bmatrix} = \begin{bmatrix} F \\ \tau \end{bmatrix} \quad (4)$$

Where:

$I \in \mathcal{R}^{(3 \times 3)}$: the inertia matrix	ω : the body angular speed
$\begin{bmatrix} I_{xx} & 0 & 0 \\ 0 & I_{yy} & 0 \\ 0 & 0 & I_{zz} \end{bmatrix}$	$\begin{bmatrix} \omega_x \\ \omega_y \\ \omega_z \end{bmatrix}$

$I_{3 \times 3} \in \mathcal{R}^{(3 \times 3)} : \text{the unity matrix}$ $\begin{bmatrix} 1 & 0 & 0 \\ 0 & 1 & 0 \\ 0 & 0 & 1 \end{bmatrix}$	$F : \text{the forces vector}$ $\begin{bmatrix} F_x \\ F_y \\ F_z \end{bmatrix}$
$V : \text{the body translational speed vector}$ $\begin{bmatrix} V_x \\ V_y \\ V_z \end{bmatrix}$	$\tau : \text{the moments vector}$ $\begin{bmatrix} \tau_x \\ \tau_y \\ \tau_z \end{bmatrix}$
$m : \text{the total mass}$	

3.3.1 The forces and moments acting on the Quadrotor

The quadrotor is an underactuated mechanical system with 6 DOF and only 4 actuators. The main forces and moments acting on it are those produced by the propellers. They can greatly vary depending on the flight regime due to their aerodynamic nature. As we consider only hovering flight, we can assume that the thrust and the drag are proportional to the square of the propellers rotation speed [3]. Thus we have:

$$T_i = b\Omega_i^2 \quad \rightarrow \quad \text{The thrust} \quad (5)$$

$$D_i = d\Omega_i^2 \quad \rightarrow \quad \text{The drag moment} \quad (6)$$

Forces:

From (4), and by neglecting $\omega \times mV$ as assumed before (R), one can get the expression of the forces acting on the quadrotor expressed in B and transformed to E :

$$RF_b = -mgE_z + R \sum_{i=1}^4 T_i \quad (7)$$

Moments:

From (4), and after adding the effect of the propellers (spinning masses) one can get the expression of the moments acting on the quadrotor expressed in B :

$$\begin{aligned} \tau_a &= \left(\tau_{ctrl_roll}, \tau_{ctrl_pitch}, \tau_{ctrl_yaw} \right)^T \\ \tau_g &= \sum_{i=1}^4 J_R (\omega \times E_z) \Omega_i \\ \tau_b &= I_{xx,yy,zz} \dot{\omega} + \omega \times I_{xx,yy,zz} \omega + \tau_g + \tau_a \end{aligned} \quad (8)$$

One can rewrite the translational and rotational dynamics as follows:

Translational dynamics:

$$\begin{cases} m \ddot{X} = (\cos \phi \sin \theta \cos \psi + \sin \phi \sin \psi) \sum_{i=1}^4 T_i \\ m \ddot{Y} = (\cos \phi \sin \theta \sin \psi - \sin \phi \cos \psi) \sum_{i=1}^4 T_i \\ m \ddot{Z} = -g + (\cos \phi \cos \theta) \sum_{i=1}^4 T_i \end{cases} \quad (9)$$

Rotational dynamics:

$$\begin{cases} I_{xx} \ddot{\phi} = \dot{\theta} \dot{\psi} (I_{yy} - I_{zz}) - J_R \dot{\theta} \Omega + \tau_{ctrl_roll} \\ I_{yy} \ddot{\theta} = \dot{\phi} \dot{\psi} (I_{zz} - I_{xx}) + J_R \dot{\phi} \Omega + \tau_{ctrl_pitch} \\ I_{zz} \ddot{\psi} = \dot{\phi} \dot{\theta} (I_{xx} - I_{yy}) + \tau_{ctrl_yaw} \end{cases} \quad (10)$$

Where:

$$\tau_a = \begin{pmatrix} \tau_{ctrl_roll} \\ \tau_{ctrl_pitch} \\ \tau_{ctrl_yaw} \end{pmatrix} = \begin{pmatrix} T_4 - T_2 \\ T_3 - T_1 \\ -D_1 + D_2 - D_3 + D_4 \end{pmatrix} \quad (11)$$

$I \in \mathfrak{R}^{(3 \times 3)}$ and $J_R \in \mathfrak{R}$ are respectively the inertia matrix and the rotor rotational inertia.

From the above model, one can see that the translational dynamics depend only on the resultant thrust vector. While the rotational dynamics are composed of:

$-\omega \times I \omega$	\rightarrow	The gyroscopic effect due to rigid body rotation
$I_R(\omega, \Omega_i)$	\rightarrow	The gyroscopic effect due to propellers change in orientation
τ_a	\rightarrow	The control moment (generated by the actuators)

Finally, the model can be rewritten in the following form, directly usable (after verification of its parameters) in simulation and control:

$$\begin{cases}
\ddot{x} = (\cos \phi \sin \theta \cos \psi + \sin \phi \sin \psi) \frac{1}{m} U_1 \\
\ddot{y} = (\cos \phi \sin \theta \sin \psi - \sin \phi \cos \psi) \frac{1}{m} U_1 \\
\ddot{z} = -g + (\cos \phi \cos \theta) \frac{1}{m} U_1 \\
\ddot{\phi} = \dot{\theta} \dot{\psi} \left(\frac{I_{yy} - I_{zz}}{I_{xx}} \right) - \frac{J_R}{I_{xx}} \dot{\theta} \Omega + \frac{l}{I_{xx}} U_2 \\
\ddot{\theta} = \dot{\phi} \dot{\psi} \left(\frac{I_{zz} - I_{xx}}{I_{yy}} \right) + \frac{J_R}{I_{yy}} \dot{\phi} \Omega + \frac{l}{I_{yy}} U_3 \\
\ddot{\psi} = \dot{\phi} \dot{\theta} \left(\frac{I_{xx} - I_{yy}}{I_{zz}} \right) + \frac{1}{I_{zz}} U_4
\end{cases} \quad (12)$$

The control inputs are simply the forces and moments produced by the four motors:

$$\begin{cases}
U_1 = b(\Omega_1^2 + \Omega_2^2 + \Omega_3^2 + \Omega_4^2) \\
U_2 = b(\Omega_4^2 - \Omega_2^2) \\
U_3 = b(\Omega_3^2 - \Omega_1^2) \\
U_4 = d(\Omega_2^2 + \Omega_4^2 - \Omega_1^2 - \Omega_3^2) \\
\Omega = -\Omega_1 + \Omega_2 - \Omega_3 + \Omega_4
\end{cases} \rightarrow \begin{cases}
U_1: \text{Vertical thrust resultant force} \\
U_2: \text{Roll moment} \\
U_3: \text{Pitch moment} \\
U_4: \text{Yaw moment} \\
\Omega: \text{Disturbance}
\end{cases} \quad (13)$$

Actuators dynamics:

In fact, this model represents the dynamics of the whole quadrotor except the dynamics of the actuators. This should not be a problem if the actuators dynamics are negligible (fast) or if the system is very slow. However, in the case of the helicopter, one needs to include these dynamics for proper simulation. In the case of a DC motor based actuator (our case); it was proved that a simple first order model is a reasonable approximation.

Symbol	Nomenclature
R	Rotation matrix
ϕ	Roll angle
θ	Pitch angle
ψ	Yaw angle
Ω	Rotor speed
$I_{xx} \ I_{yy} \ I_{zz}$	Body inertias
J_R	Rotor inertia
b	Thrust factor
d	Drag factor

3.4 Open-loop behavior

After taking a short look to the dynamic model developed above, one can see a combination of two gyroscopic effects. The first one is due to rigid body rotation and the second one is due to the change in orientation of the propeller rotation (change in orientation of the kinetic momentum) [6]. As a response to an initial roll or pitch angular speed, the system tends to amplify these effects naturally as shown in Fig. 6.

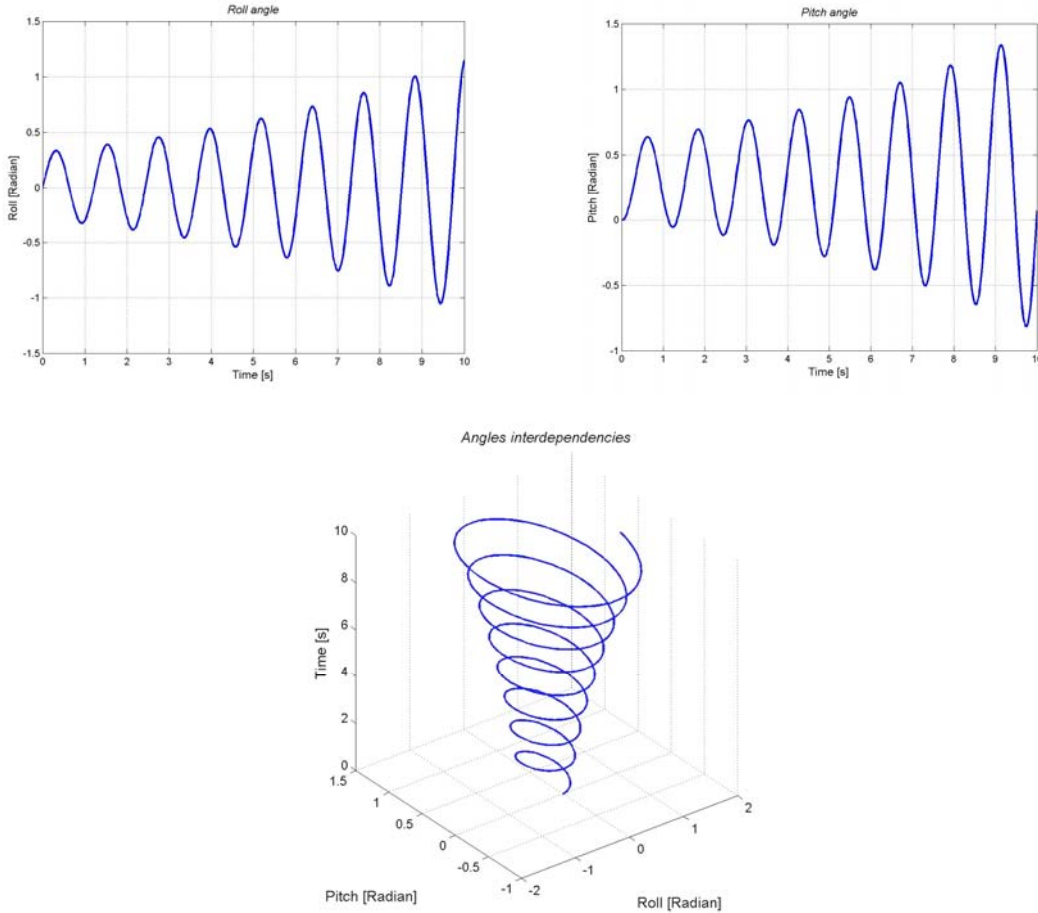


Figure 6: Natural response of the roll, pitch angles and their interdependencies

This highly unstable behavior is mainly due to the gyroscopic effect due to the change in orientation of the propeller axis of rotation. In fact, the influence of the rotational inertia of the propeller becomes relatively high comparing to the overall inertia of the system.

3.5 Closed-loop behavior with PID controller

As we saw it in the previous chapter, the helicopter is a highly instable system. We will show here the implementation of a basic PID controller [4][7]:

$$U_1 = b(\Omega_1^2 + \Omega_2^2 + \Omega_3^2 + \Omega_4^2) = 2.4 \text{ N (weight of the system)} \quad (14)$$

$$U_2 = b(\Omega_2^2 - \Omega_4^2) = k_\phi(\phi_d - \phi) + d_\phi(\dot{\phi}_d - \dot{\phi}) \quad (15)$$

$$U_3 = b(\Omega_3^2 - \Omega_1^2) = k_\theta(\theta_d - \theta) + d_\theta(\dot{\theta}_d - \dot{\theta}) \quad (16)$$

$$U_4 = d(-\Omega_2^2 - \Omega_4^2 + \Omega_1^2 + \Omega_3^2) = k_\psi(\psi_d - \psi) - d_\psi(\dot{\psi}_d - \dot{\psi}) \quad (17)$$

This controller doesn't take into account the gyroscopic effects but only the effects of propellers thrusts and drag. This controller is thus valid only in near hover situation.

With the appropriate proportional and derivative terms, this controller stabilizes roll, pitch and yaw of the system as shown in the figures below.

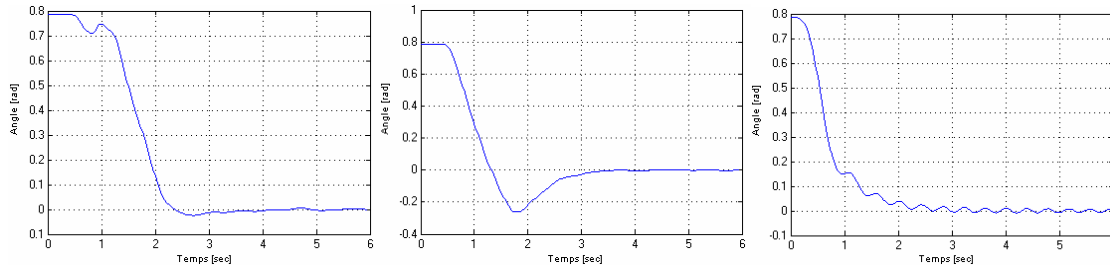


Figure 7: Roll, pitch and yaw with PD regulator on simulation
($K_p=0.8$ $T_d=0.4$ for roll/pitch $K_p=0.8$ $T_d=0.5$ for yaw)

On the real model, the gains, especially for yaw, have to be adapted as the motors were near saturation.

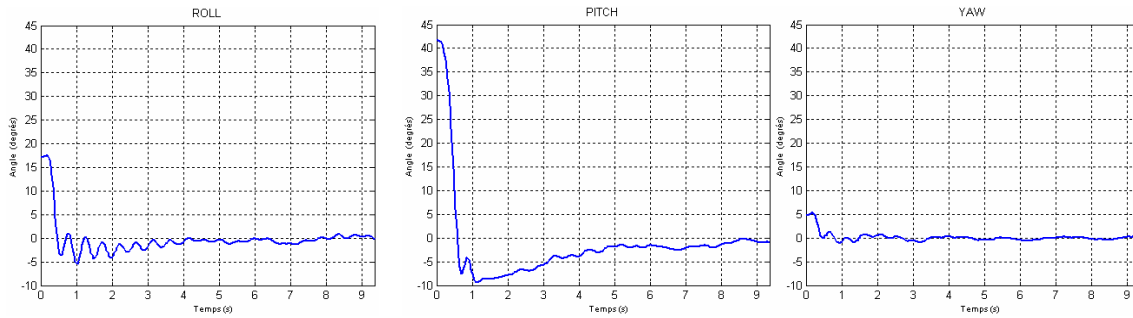


Figure 8: Roll, pitch and yaw with PID regulator on the real helicopter
($K_p=0.9$ $T_d=0.2$ $T_i=0.3$ for roll/pitch $K_p=0.06$ $T_d=0.02$ $T_i=0.3$ for yaw)

Moreover, an integral term was needed. In fact, on the real model there are little imperfections like different thrust coefficient for propellers, small dissymmetry, etc. which will induce a small constant error. That's why it's important integrates this error and include it in the control.

4 The Airplane example

Depending on the final applications, the configurations of an airplane, i.e its dimensions, aerodynamics, propulsion system and controls, are very different from one model to another. In fact, the design of a mono-place acrobatic aircraft will completely differ compared to a jet airplane that can transport more than 400 passengers. Anyway, in both cases the principles of flight are the same.

The example presented here is the model-scale solar airplane Sky-Sailor that is intended to achieve continuous flight with the only energy of the sun. It consists of a glider with a wingspan of 3.2 meters that is motorized by a DC motor connected to the propeller (a) through a gearbox. The control surfaces are:

- Two ailerons (b) on the main wing that act mainly on the roll of the airplane
- The V-tail (c) at the rear side composed of two control surfaces that act mainly on the pitch if they change symmetrically (elevator) and on the yaw if their deviation is not symmetrical (rudder).

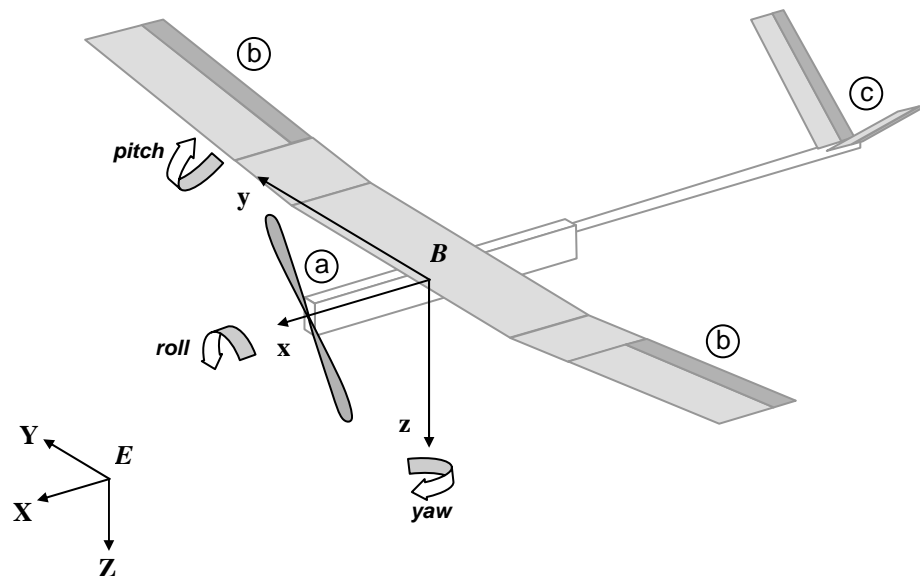


Figure 9: The controls on Sky-Sailor are the propeller, the ailerons and the V-tail that mixes rudder and elevator

4.1 Dynamic modeling

The forces acting on the airplane are mainly:

- the weight $m \cdot g$ located at the center of gravity
- the thrust of the propeller acting in the x direction. Modeling a propeller is a very complex task, that is the reason why values measured by experiments will be taken.
- the aerodynamic forces of each part of the airplane, mainly the wing and the V-tail. Here, the theory is simpler and will be topic of the next chapter.

4.2 Aerodynamic forces of an airfoil

The figure below shows the section of a wing also called airfoil. The chord of the wing is the line between the leading and the trailing edge and the angle between the relative speed and this chord is the angle of attack (Aoa).

As every other solid moving in a fluid at a certain speed, one can represent the sum of all aerodynamic forces acting on the wing with two perpendicular forces: the lift force F_l and the drag force F_d that are respectively perpendicular and parallel to the speed vector.

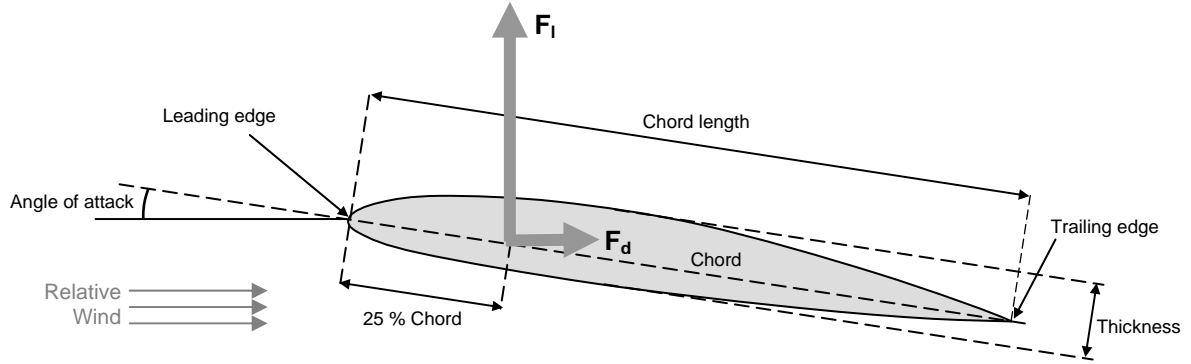


Figure 10: Section of the wing (airfoil) and the lift and drag forces

The application point of the lift and drag forces is very close to the 25% of the chord but this can slightly change depending on the angle of attack. In order to simplify the problem, the application point is considered as fixed and a moment is added to correct this assumption.

$$F_l = C_l \frac{\rho}{2} S v^2 \quad (18)$$

$$F_d = C_d \frac{\rho}{2} S v^2 \quad (19)$$

$$M = C_m \frac{\rho}{2} S v^2 \cdot \text{chord} \quad (20)$$

with ρ : Density of fluid (air)
 S : Wing area
 v : Flight speed (relative to surrounding fluid)
 C_L : Lift coefficient
 C_D : Drag coefficient
 C_M : Moment coefficient

The lift, drag and moment coefficients depend on the airfoil, the angle of attack and a third value that is the Reynolds number. It is representative of the viscosity of the fluid but will not be explained more in details. C_l increases almost linearly with the angle of attack until

the stall angle is reached. The wing should never work in this zone where the C_l decreases importantly which makes the airplane losing altitude very rapidly. C_d has a quadratic relation to the angle of attack.

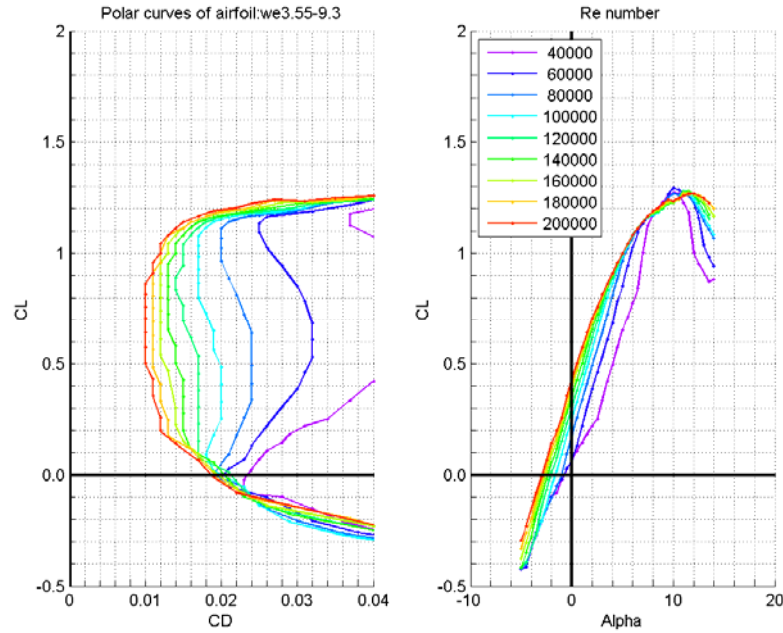


Figure 11: Lift and drag coefficients of Sky-Sailor airfoil

4.3 Modeling assumptions

The airplane is considered as a rigid body associated with the aerodynamic forces generated by the propeller and the wing.

- The center of mass and the body fixed frame origin are assumed to coincide.
- The structure is supposed rigid and symmetric (diagonal inertia matrix).
- The drag force of the fuselage is neglected
- The wind speed in the Earth frame is set to zero so that the relative wind on the body frame is only due to the airplane speed.
- The relative wind induced by the rotation of the airplane is neglected

4.4 Model derivation using Lagrange-Euler approach

The Lagrange-Euler approach is based on the concept of kinetic and potential energy:

$$\Gamma_i = \frac{d}{dt} \left(\frac{\partial L}{\partial \dot{q}_i} \right) - \frac{\partial L}{\partial q_i} \quad (21)$$

$$L = T - V \quad (22)$$

avec q_i : generalized coordinates

Γ_i : generalized forces given by non-conservatives forces

T : total kinetic energy

V : total potential energy

The kinetic energy due to the translation is immediately:

$$E_{cin translation} = \frac{1}{2} m \dot{x}^2 + \frac{1}{2} m \dot{y}^2 + \frac{1}{2} m \dot{z}^2 \quad (23)$$

As we state it in the hypothesis, we assume that the inertia matrix is diagonal and thus, that the inertia products are null. The kinetic energy due to the rotation is:

$$E_{cin rotation} = \frac{1}{2} I_{xx} \omega_x^2 + \frac{1}{2} I_{yy} \omega_y^2 + \frac{1}{2} I_{zz} \omega_z^2 \quad (24)$$

Where $\omega_x, \omega_y, \omega_z$ are the rotational speed that can be expressed as a function of the roll, pitch and yaw rate $(\dot{\phi}, \dot{\theta}, \dot{\psi})$:

$$\begin{pmatrix} \omega_x \\ \omega_y \\ \omega_z \end{pmatrix} = \begin{pmatrix} \dot{\phi} - \dot{\psi} \cdot \sin \theta \\ \dot{\theta} \cdot \cos \phi + \dot{\psi} \cdot \sin \phi \cos \theta \\ -\dot{\theta} \cdot \sin \phi + \dot{\psi} \cdot \cos \phi \cos \theta \end{pmatrix} \quad (25)$$

This leads to the total kinetic energy:

$$T = \frac{1}{2} (m \dot{x}^2 + m \dot{y}^2 + m \dot{z}^2 + I_{xx} \omega_x^2 + I_{yy} \omega_y^2 + I_{zz} \omega_z^2) \quad (26)$$

The potential energy can be expressed by:

$$V = -m \cdot g \cdot Z = -m \cdot g \cdot (-\sin \theta \cdot x + \sin \phi \cos \theta \cdot y + \cos \phi \cos \theta \cdot z) \quad (27)$$

The Lagrangian is :

$$L = T - V \quad (28)$$

The motion equations are then given by:

$$\frac{d}{dt} \left(\frac{\partial L}{\partial \dot{x}} \right) - \frac{\partial L}{\partial x} = F_x \quad \frac{d}{dt} \left(\frac{\partial L}{\partial \dot{y}} \right) - \frac{\partial L}{\partial y} = F_y \quad \frac{d}{dt} \left(\frac{\partial L}{\partial \dot{z}} \right) - \frac{\partial L}{\partial z} = F_z \quad (29)$$

$$\frac{d}{dt} \left(\frac{\partial L}{\partial \dot{\psi}} \right) - \frac{\partial L}{\partial \psi} = \tau_{\psi} \quad \frac{d}{dt} \left(\frac{\partial L}{\partial \dot{\phi}} \right) - \frac{\partial L}{\partial \phi} = \tau_{\phi} \quad \frac{d}{dt} \left(\frac{\partial L}{\partial \dot{\theta}} \right) - \frac{\partial L}{\partial \theta} = \tau_{\theta} \quad (30)$$

After calculation, we obtain the left parts of equations above:

$$\frac{d}{dt} \left(\frac{\partial L}{\partial \dot{x}} \right) - \frac{\partial L}{\partial x} = m \ddot{x} + mg \sin \theta \quad (31)$$

$$\frac{d}{dt} \left(\frac{\partial L}{\partial \dot{y}} \right) - \frac{\partial L}{\partial y} = m \ddot{y} - mg \sin \phi \cos \theta \quad (32)$$

$$\frac{d}{dt} \left(\frac{\partial L}{\partial \dot{z}} \right) - \frac{\partial L}{\partial z} = m \ddot{z} - mg \cos \phi \cos \theta \quad (33)$$

$$\frac{d}{dt} \left(\frac{\partial L}{\partial \dot{\phi}} \right) - \frac{\partial L}{\partial \phi} = I_{xx} \dot{\omega}_x - (I_{yy} - I_{zz}) \omega_y \omega_z \quad (34)$$

$$\begin{aligned} \frac{d}{dt} \left(\frac{\partial L}{\partial \dot{\theta}} \right) - \frac{\partial L}{\partial \theta} = & -\sin \phi (\dot{\omega}_z I_{zz} - \omega_x \omega_y (I_{xx} - I_{yy})) \\ & + \cos \phi (\dot{\omega}_y \cdot I_{yy} - \omega_x \omega_z (I_{zz} - I_{xx})) \end{aligned} \quad (35)$$

$$\begin{aligned} \frac{d}{dt} \left(\frac{\partial L}{\partial \dot{\psi}} \right) - \frac{\partial L}{\partial \psi} = & -\sin \theta \cdot (\dot{\omega}_x I_{xx} - \omega_y \omega_z (I_{yy} - I_{zz})) \\ & + \sin \phi \cos \theta \cdot (\dot{\omega}_y I_{yy} - \omega_x \omega_z (I_{zz} - I_{xx})) \\ & + \cos \phi \cos \theta \cdot (\dot{\omega}_z I_{zz} - \omega_x \omega_y (I_{xx} - I_{yy})) \end{aligned} \quad (36)$$

The non-conservative forces and moments come from the aerodynamics. On the airplane, seven parts are considered as depicted on the figure below where the right and left side of are divided into a portion with and without control surface.

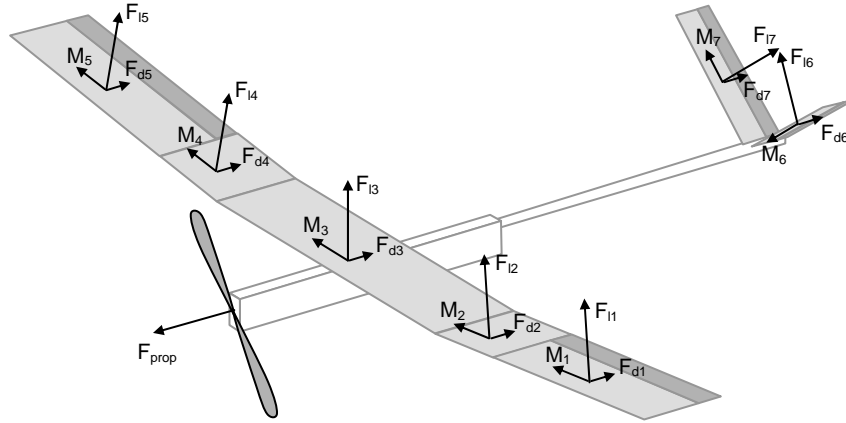


Figure 12: Forces and moments on the airplane

$$\begin{aligned} F_{tot} &= F_{prop} + \sum_{i=1}^7 F_{Li} + F_{di} \\ M_{tot} &= \sum_{i=1}^7 M_i + F_{Li} \times r_i + F_{di} \times r_i \end{aligned}$$

$$\left| \begin{aligned} F_{prop} &= f(\dot{x}, U_1) \\ F_{li} &= C_{li} \frac{\rho}{2} S_i v^2 \\ F_{di} &= C_{di} \frac{\rho}{2} S_i v^2 \\ M_i &= C_{mi} \frac{\rho}{2} S_i v^2 \cdot chord_i \end{aligned} \right. \quad (37)$$

$$\left\{ \begin{array}{l} [C_{l1} \ C_{d1} \ C_{m1}] = f(Aoa_i, U_2) \\ [C_{li} \ C_{di} \ C_{mi}] = f(Aoa_i) \quad \text{for } i=2,3,4 \\ [C_{l5} \ C_{d5} \ C_{m5}] = f(Aoa_i, U_3) \\ [C_{l6} \ C_{d6} \ C_{m6}] = f(Aoa_i, U_4) \\ [C_{l7} \ C_{d7} \ C_{m7}] = f(Aoa_i, U_5) \end{array} \right. \quad (38)$$

U_1 to U_5 are the control inputs: U_1 is the voltage on the motor and U_2, U_3, U_4, U_5 are respectively the deflection of the left aileron, the right aileron, the left V-tail and the right V-tail.

Final model with small angle approximation

Isolating the acceleration and applying the small angle approximation, where the rotational speed in the solid basis are equal to Euler's angles rates, we obtain:

$$\left\{ \begin{array}{l} \ddot{x} = \frac{F_{tot,x}}{m} - g \sin \theta \\ \ddot{y} = \frac{F_{tot,y}}{m} + g \sin \phi \cos \theta \\ \ddot{z} = \frac{F_{tot,z}}{m} + g \cos \phi \cos \theta \\ \ddot{\phi} = \frac{I_{yy} - I_{zz}}{I_{xx}} \dot{\psi} \dot{\theta} + \frac{M_{tot,x}}{I_{xx}} \\ \ddot{\theta} = \frac{I_{zz} - I_{xx}}{I_{yy}} \dot{\psi} \dot{\phi} + \frac{M_{tot,y}}{I_{yy}} \\ \ddot{\psi} = \frac{I_{xx} - I_{yy}}{I_{zz}} \dot{\theta} \dot{\phi} + \frac{M_{tot,z}}{I_{zz}} \end{array} \right. \quad \text{or in Earth frame} \quad \left\{ \begin{array}{l} \ddot{X} = \frac{F_{tot,X}}{m} \\ \ddot{Y} = \frac{F_{tot,Y}}{m} \\ \ddot{Z} = \frac{F_{tot,Z}}{m} + g \\ \ddot{\phi} = \frac{I_{yy} - I_{zz}}{I_{xx}} \dot{\psi} \dot{\theta} + \frac{M_{tot,x}}{I_{xx}} \\ \ddot{\theta} = \frac{I_{zz} - I_{xx}}{I_{yy}} \dot{\psi} \dot{\phi} + \frac{M_{tot,y}}{I_{yy}} \\ \ddot{\psi} = \frac{I_{xx} - I_{yy}}{I_{zz}} \dot{\theta} \dot{\phi} + \frac{M_{tot,z}}{I_{zz}} \end{array} \right. \quad (39)$$

Note that only the angular dynamics were developed using the Lagrangian approach.

4.5 Open-Loop behavior

The simulation of the airplane shows a good stability in open loop, this means if the motor is turned off and all the deflection of the ailerons are set to zero. This behavior of natural stabilization was also tested on the real airplane during experiments.

The following figure shows the evolution of the airplane that start with a pitch angle of 0.2 rad (11.5°). One can see that after 40 seconds, the airplane is quite stable. With horizontal and vertical speeds of 8.2, respectively 0.32 [m/s], we obtain a glide slope of 25.6 which is very close to the reality.

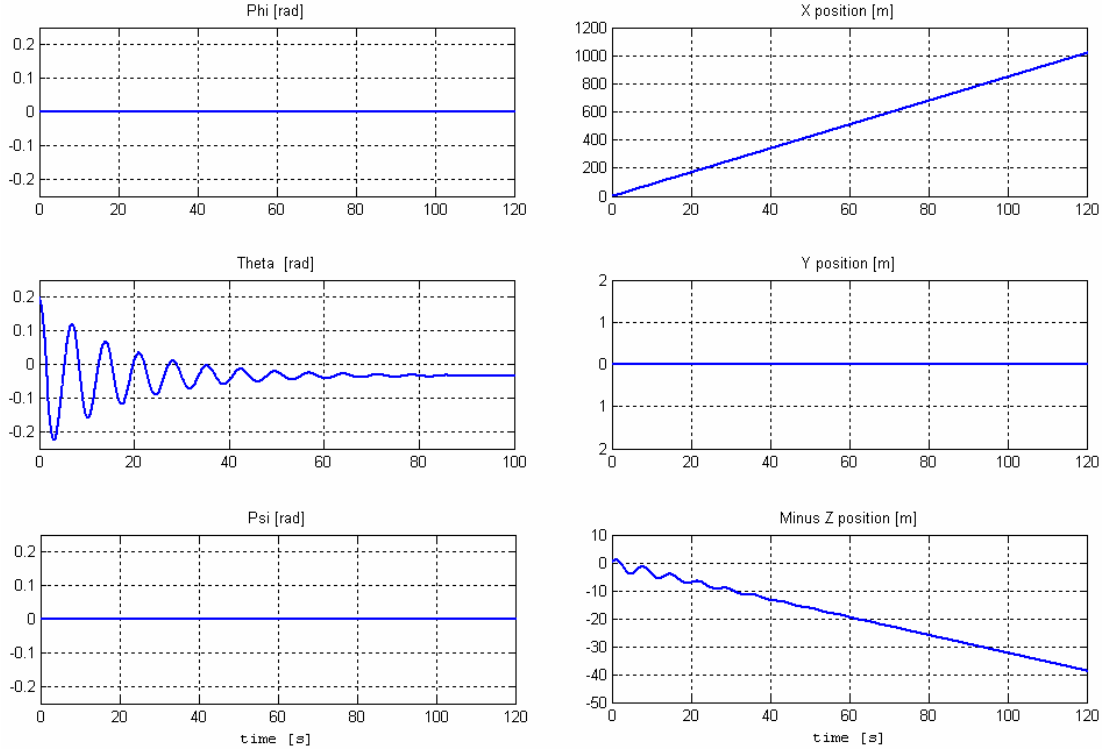


Figure 13: Open-loop behavior with an initial pitch of 0.2 rad

5 Model verification

Both of the models developed above contain physical parameters which must be known with good precision.

For the helicopter, there are m , I_{xx} , I_{yy} , I_{zz} , b and d . These values are directly measured when it is possible to do so, for instance the mass m that is obtained by direct weighing, but others like the inertias are obviously harder to measure. Here it is possible to have a preliminary estimation directly from a CAD model if it is similar to the real construction. Usually, an identification algorithm is run by exiting the system with a special signal. However, this is more complex in the case of unstable systems like the helicopter.

For the model of the airplane, these parameters are also m , I_{xx} , I_{yy} , I_{zz} and all the aerodynamic coefficients C_{li} , C_{di} , C_{mi} that depends on the speed and the angle of attack. There exist software that allow a calculation of these values but the better way is for sure a direct measurement of the forces and the torques on a piece of the wing placed in a wind tunnel.

6 References

- [1] <http://asl.epfl.ch/>
- [2] R.M. Murray, Z. Li, and S.S. Sastry, A mathematical introduction to robotic manipulation. CRC Press, 1994.
- [3] S. Bouabdallah, P. Murrieri and R. Siegwart, Design and Control of an Indoor Micro Quadrotor. ICRA 2004, New Orleans (USA), April 2004.
- [4] S. Bouabdallah, A. Noth and R. Siegwart, PID vs LQ Control Techniques Applied to an Indoor Micro Quadrotor. IROS 2004, Sendai (Japan), October 2004.
- [5] R. Olfati-Saber, Nonlinear Control of Underactuated Mechanical Systems with Application to Robotics and Aerospace Vehicles. Phd thesis, Department of Electrical Engineering and Computer Science, MIT, 2001.
- [6] H. Baruh, Analytical Dynamics. McGraw-Hill, 1999.
- [7] A. Noth, Synthèse et Implémentation d'un Contrôleur pour Micro Hélicoptère à 4 Rotors, Diploma Project 2004.
- [8] Robert F. Stengel, Flight dynamics. Princeton University Press, 2004.
- [9] A. Noth, W. Engel, R. Siegwart, Design of an Ultra-Lightweight Autonomous Solar Airplane for Continuous Flight. In Proceedings of Field and Service Robotics, Port Douglas, Australia, 2005.
- [10] <http://www.mh-aerotools.de/airfoils/javafoil.htm>
- [11] http://en.wikipedia.org/wiki/Tait-Bryan_angles